55.8 (porphyrin-CH_2-CH_2-N), 70.8, 71.2 (N-CH_2-CH_2O), 95.5, 95.7 (meso C), 134.3, 135.2, 136.8, 141.9 (pyrrole β C), 143.0, 145.1 (pyrrole α C). λ_{max} 388 nm. Anal. Calcd for $C_{88}H_{120}N_{12}O_8$: C, 71.71; H, 8.21; N, 11.40. Found: C, 71.90; H, 8.12; N, 11.39. *m/e* 1473 (calcd 1473).

Zn Biphenyl-C_2-porphyrin Bis-[18]-N_2O_4 Macrotetracyclic Complex 19. The free-base porphyrin **1** (10 mg, 0.0085 mmol) was dissolved in 10 mL of hot CH_2Cl_2, and 0.89 mL of a 0.010 N solution of zinc acetate in CH_3OH was added. When, as judged by the absence of bands at 497 *nm* 619 nm in the visible spectrum, the reaction was considered complete, the pink solution was poured into a very dilute aqueous solution of LiOH. The organic layer was separated off, and the aqueous phase was extracted with $CHCl_3$ (2 × 20 mL). The organic phases were combined, dried over $MgSO_4$, and taken to dryness in vacuo to yield **19** (10.2 mg, 97%). ^1H NMR ($CDCl_3$): no peaks associated with the pyrrole N–H protons are observed; other features were similar to those observed for the free-base **1**. λ_{max} 405 nm.

Zn Biphenyl-C_3-porphyrin Bis-[18]-N_2O_4 Macrotetracyclic Complex 20 was prepared from **2** by the same procedure used to prepare **19** from **1**. For 10 mg (0.0083 mmol) of the free-base, 0.90 mL of the stock 0.010 N zinc acetate solution was used to give 10 mg (95%) of the zinc complex **20**. ^1H NMR ($CDCl_3$): no signals ascribable to a pyrrolic N–H are detected; other features much as for the free-base. λ_{max} 402 nm.

Zn_2 Bis-C_2-porphyrin Bis-[18]-N_2O_4 Dinuclear Macropentacyclic Complex 22 was prepared in 97% yield from **3** by using a similar procedure. For 10 mg of the free-base **3**, 1.42 mL of the 0.010 N zinc acetate stock solution was used to give 10.5 mg of the bis-zinc complex **22**. ^1H NMR ($CDCl_3$): no signals ascribable to a pyrrolic N–H were observed; other features much as for the free-base. λ_{max} 385 nm.

Cu Biphenyl-C_2-porphyrin Bis-[18]-N_2O_4 Macrotetracyclic Complex 21. The purified free-base compound, **1** (50 mg, 0.043 mmol), was dissolved in $CHCl_3$ (20 mL) at 40 °C, and 5 mL of a saturated solution of copper acetate in CH_3OH were added. After approximately 10 min, when visible spectroscopy indicated the absence of starting material (no bands were observed at 497 and 619 nm), the reaction mixture was poured into a 0.1 N aqueous solution of NaCN, made slightly basic by the addition of LiOH. The organic layer was extracted out, washed with water (3 × 20 mL), dried over Na_2SO_4, and stripped to dryness on a rotary evaporator. Recrystallization from CH_2Cl_2–hexane yielded the copper complex **21** as large purple crystals (50 mg, 95%). λ_{max} 399 nm. Anal. Calcd for $C_{70}H_{99}N_8O_8Cu \cdot 2H_2O$: C, 65.94; H, 7.75. Found: C, 66.24; H, 7.81. This compound was also characterized by an X-ray crystallographic structure determination.[20]

Cu_2 Bis-C_2-porphyrin Bis-[18]-N_2O_4 Dinuclear Macropentacyclic Complex 23 was prepared in an identical manner as above from the free-base **3** in 92% yield. λ_{max} 390 nm. The crystals obtained were kept in view of an X-ray crystallographic analysis. Anal. Calcd for $C_{88}H_{116}N_{12}O_8Cu_2 \cdot 5H_2O$: C, 62.65; H, 7.53; N, 9.96. Found: C, 62.69; H, 7.22; N, 9.62.

Acknowledgment. The authors thank Merck A.G., Darmstadt, for the gift of the [18]-N_2O_4 macrocycle **12** used in this work. A.D.H. and J.L.S. thank both the NATO and NSF–CNRS scientific exchange programmes for postdoctoral research fellowships.

Registry No. 1, 90633-79-7; **1**·$^+H_3N(CH_2)_8NH_3^+$, 103201-89-4; **1**·$^+H_3N(CH_2)_9NH_3^+$, 90633-81-1; **1**·$^+H_3N(CH_2)_{10}NH_3^+$, 103201-90-7; **2**, 90633-80-0; **2**·$^+H_3N(CH_2)_8NH_3^+$, 103201-91-8; **2**·$^+H_3N(CH_2)_9NH_3^+$, 90633-82-2; **2**·$^+H_3N(CH_2)_{10}NH_3^+$, 103201-92-9; **3**, 90653-21-7; **3**·$^+H_3N(CH_2)_8NH_3^+$, 103201-93-0; **3**·$^+H_3N(CH_2)_9NH_3^+$, 90653-22-8; **3**·$^+H_3N(CH_2)_{10}NH_3^+$, 103201-94-1; **6**, 74427-71-7; **9**, 90653-18-2; **10**, 90633-76-4; **10** (Zn complex), 103201-95-2; **11**, 90633-77-5; **12**, 23978-55-4; **13**, 2351-37-3; **14**, 42031-79-8; **15**, 90633-73-1; **16**, 90653-20-6; **16** (Zn complex), 103201-96-3; **17**, 90633-78-6; **18**, 90653-19-3; **19**, 90603-80-8; **19**·$^+H_3N(CH_2)_8NH_3^+$, 90818-88-5; **19**·$^+H_3N(CH_2)_9NH_3^+$, 90818-90-9; **19**·$^+H_3N(CH_2)_{10}NH_3^+$, 90818-89-5; **20**, 90603-81-9; **20**·$^+H_3N(CH_2)_8NH_3^+$, 90822-43-8; **20**·$^+H_3N(CH_2)_9NH_3^+$, 90818-90-9; **20**·$^+H_3N(CH_2)_{10}NH_3^+$, 90818-91-8; **21**, 103201-97-4; **22**, 90603-82-0; **22**·$^+H_3N(CH_2)_8NH_3^+$, 90818-92-1; **22**·$^+H_3N(CH_2)_9NH_3^+$, 90818-93-2; **22**·$^+H_3N(CH_2)_{10}NH_3^+$, 90818-94-3; **23**, 103201-98-5; $^+H_3N(CH_2)_8NH_3^+$, 49745-06-4; $^+H_3N(CH_2)_9NH_3^+$, 103201-88-3; $^+H_3N(CH_2)_{10}NH_3^+$, 49745-07-5.

The Mechanism of Nickel-Catalyzed Ethylene Hydrocyanation. Reductive Elimination by an Associative Process

Ronald J. McKinney* and D. Christopher Roe*

Contribution No. 3765 from the Central Research and Development Department, E. I. du Pont de Nemours and Company, Experimental Station, Wilmington, Delaware 19898. *Received February 13, 1986*

Abstract: The complex $(C_2H_4)L(CN)(C_2H_5)Ni^{II}$ [L = P(O-*o*-tolyl)$_3$] has been identified at −40 °C by ^1H, ^{31}P, and ^{13}C NMR spectroscopy as the primary intermediate in the catalytic hydrocyanation of ethylene. Reaction of this intermediate with L causes reductive elimination of propanenitrile and produces $(C_2H_4)L_2Ni$ which reacts with ethylene and hydrogen cyanide to regenerate the intermediate. Measurements of second-order rate constants at −50 to −10 °C result in $\Delta H^\ddagger$ = 8.8 ± 0.9 kcal/mol and $\Delta S^\ddagger$ = −34 ± 4 eu ($\Delta G^\ddagger$ = 16.7 ± 0.1 kcal/mol at −40 °C). At higher L concentrations, these nickel species are also in equilibrium with $(C_2H_4)L_3Ni$, L_4Ni, and $HNi(CN)L_3$ which remove nickel from the productive catalytic cycle. Equilibrium constants relating these species and corresponding thermodynamic parameters have been determined. The rates of dissociation of L from L_4Ni and $HNi(CN)L_3$ have also been determined. The former reaction is very slow with $\Delta H^\ddagger$ = 20.1 ± 1.6 kcal/mol and $\Delta S^\ddagger$ = 7 ± 7 eu ($\Delta G^\ddagger$ = 18.5 kcal/mol at −40 °C) whereas the latter is about 10^3 faster with $\Delta H^\ddagger$ = 18.8 ± 2.7 kcal/mol and $\Delta S^\ddagger$ = 17 ± 10 eu ($\Delta G^\ddagger$ = 14.8 kcal/mol at −40 °C).

The development of the Du Pont adiponitrile process,[1] i.e., the dihydrocyanation of butadiene, has provided on the one hand a remarkable example of industrial application of homogeneous catalysis and on the other an excellent opportunity for detailed mechanistic studies of a complex practical system. A series of recent reports from our laboratories,[2-11] as well as others,[12-17] is developing a general picture of nickel-catalyzed olefin hydrocyanation.[18,19] However, understanding of many of the funda-

(1) *Chem. Eng. New* **1971**, *49*, 30.
(2) (a) Tolman, C. A.; Seidel, W. C.; Gosser, L. W. *J. Am. Chem. Soc.* **1974**, *96*, 53. (b) Gosser, L. W.; Tolman, C. A. *Inorg. Chem.* **1970**, *9*, 2350.
(3) Druliner, J. D.; English, A. D.; Jesson, J. P.; Meakin, P.; Tolman, C. A. *J. Am. Chem. Soc.* **1976**, *98*, 2156.
(4) Tolman, C. A.; Seidel, W. C. *J. Am. Chem. Soc.* **1974**, *96*, 2774.
(5) Tolman, C. A. *J. Am. Chem. Soc.* **1974**, *96*, 2780.
(6) Tolman, C. A. *Organometallics* **1983**, *2*, 614.
(7) Tolman, C. A.; Seidel, W. C.; Gosser, L. W. *Organometallics* **1983**, *2*, 1391.
(8) Tolman, C. A. *Inorg. Chem.* **1971**, *10*, 1540.

0002-7863/86/1508-5167$01.50/0

Table I. NMR Data[a]

	^{31}P	^{1}H		
		Ar-CH_3	Ar-*o*-*H*	
$L_2(C_2H_4)Ni$ (**1**)	141.44	2.18	7.44	1.84 (C_2H_4)
$L(C_2H_4)(CN)(C_2H_5)Ni$ (**2a**)	118.09 (J_{P-C} = 41,[b] 23[c] Hz)			
(**2b**)	117.74 (J_{PC} = 39,[b] 23[c] Hz)	2.09	7.88	2.03 (C_2H_4); 0.6 (C_2H_5)
(**2c**)	116.95 (J_{P-C} = 29,[a] 142[c] Hz)			
$HNi(CN)L_3$ (**3**)	119.52	1.89		
$L_3Ni(C_2H_4)$ (**5**)	135.36	2.04	7.60	3.59 (C_2H_4)
$L_3Ni(NCCH_3)$	132.36	2.08	7.73	
L_4Ni	130.32	1.95[d]	7.67[b]	
L_3Ni	131.32[d]	1.97[d]	7.45[b]	
L	129.82	2.11[d]	7.24[b]	

[a] In toluene-d_8 at −40 °C; L = P(O-*o*-tolyl)$_3$. [b] $J_{P-CH_2CH_3}$. [c] J_{P-CN}. [d] At 30 °C.

mental steps of this complex reaction system is still lacking. Our recent efforts have focussed on understanding the apparent final step in the catalytic sequence, namely the reductive elimination of organonitrile from the nickel catalyst. In the adiponitrile process, this step is complicated by isomerization of olefins and the opportunity for hydrogen cyanide to add to an unsymmetrical olefin in two ways, thereby providing the possibility of a number of different alkyl nickel species with which to contend.[10] Recently Tolman et al.[10] reported a reaction which eliminates these complications and therefore appeared to be ideal for such an in-depth study. These authors found that the reaction of $HNi(CN)L_3$ [L = P(O-*o*-tolyl)$_3$] with ethylene at −50 °C rapidly produces a nickel species containing both ethyl and cyano ligands which then slowly eliminates propanenitrile.

In this paper, we report the characterization of an intermediate (ethyl)(cyano)nickel species by ^{1}H, ^{31}P, and ^{13}C NMR spectroscopy and kinetic and equilibrium studies relating to its catalytic behavior in the hydrocyanation of ethylene. The evidence defines a well-characterized associative pathway for reductive elimination. A preliminary account of this study has appeared.[20]

These studies are related to the more general reductive elimination of alkyl groups from metal centers as illustrated by eq 1 (R, R′ = alkyl, aryl, and hydride). This process has attracted

(1)

attention over the last 15 years because of a growing interest in stoichiometric and catalytic organometallic methods for generating new carbon–carbon bonds. The majority of studies have dealt with d^8, four-coordinate complexes of Ni(II), Pd(II), Pt(II), and Au(III). Three mechanistic pathways have been identified, the choice of which depends on both the metal and the ligands involved: (1) eliminations where the rate of reaction is unaffected by added ligands, termed "direct reductive elimination"; (2) eliminations where the rate is inhibited by the addition of ligands and which appears to proceed by prior dissociation of a ligand to generate a three-coordinate intermediate, termed "dissociative reductive elimination"; and (3) eliminations where the rate is accelerated by added ligand, a feature which strongly suggests a five-coordinate intermediate and leads to the description "associative reductive elimination". The majority of the well-documented cases belong to the first two classes with direct elimination occurring for some Ni and Pt cases[21] and dissociative elimination occurring for some Ni, Pd, and Au complexes.[22] Associative elimination is rather unusual and has been observed for Ni only in three cases,[23-25] one of which involves elimination of aryl nitrile from an (aryl)NiCN complex.[24] It is now widely accepted that a necessary but not sufficient requirement for in-

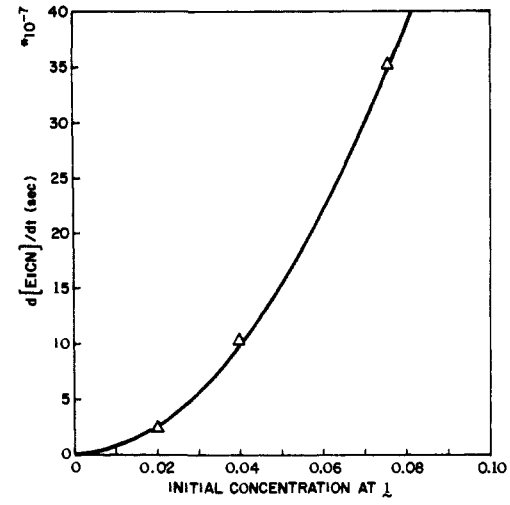

Figure 1. Rate of propanenitrile formation vs. the initial concentration of complex **1**, at −40 °C in toluene-d_8.

(9) Seidel, W. C.; Tolman, C. A. *Anal. N.Y. Acad. Sci.* **1983**, *415*, 201.
(10) Tolman, C. A.; Seidel, W. C.; Druliner, J. D.; Domaille, P. J. *Organometallics* **1984**, *3*, 33.
(11) Druliner, J. D. *Organometallics* **1984**, *3*, 205.
(12) Keim, W.; Behr, A.; Luehr, H. O. *J. Catal.* **1982**, *78*, 209.
(13) Keim, W.; Behr, A.; Broul, J. P.; Weisser, J. *ErdoeL Kohle, Erdgas, Petrochem.* **1982**, *35*, 436.
(14) Backvall, J. E.; Andel. O. S. *J. Chem. Soc., Chem. Commun.* **1981**, 1098.
(15) Jackson, W. R.; Lovel, C. G. *Aust. J. Chem.* **1982**, *35*, 2053. Jackson, W. R.; Lovel, C. G. *Tetrahedron Lett.* **1982**, 1621.
(16) Jackson, W. R.; Lovel, C. G.; Probert, M.; Elmes, P. S., private communication.
(17) Elmes, P. S.; Jackson, W. R. *Aust. J. Chem.* **1982**, *35*, 2041. Elmes, P. S.; Jackson, W. R. *J. Am. Chem. Soc.* **1979**, *101*, 6128.
(18) Tolman, C. A.; McKinney, R. J.; Seidel, W. C.; Druliner, J. D.; Stevens, W. R. *Adv. Catal.* **1985**, *33*, 1.
(19) For general reviews of hydrocyanation see: (a) Brown, E. S. *Organic Synthesis via Metal Carbonyls*; Wender, Pino, Eds.; Wiley: New York, 1977; Vol. 2. Brown, E. S. *Aspects Homogeneous Catal.* **1974**, 57. (b) James, B. R. *Comprehensive Organometallic Chemistry*; Wilkinson, G., Stone, F. G. A., Abel, E. W., Eds.; Pergamon Press: New York, 1982; Vol. 8, Chapter 51, p 353. (c) Hubert, A. J.; Puentes, E. *Catalysis in C_2 Chemistry*; Keim, W., Ed.; D. *Reidel* Publishing Co.; Dordrecht, Holland, 1983; pp 219–242.
(20) McKinney, R. J.; Roe, D. C. *J. Am. Chem. Soc.* **1985**, *107*, 261.
(21) For example, see: (a) Kohara, T.; Yamamoto, T.; Yamamoto, A. *J. Organomet. Chem.* **1980**, *192*, 265. (b) Grubbs, R. H.; Miyashita, A.; Liu, M.; Burk, P. *J. Am. Chem. Soc.* **1977**, *99*, 3868; **1978**, *100*, 2418. (c) Abis, L.; Sen, A.; Halpern, J. *J. Am. Chem. Soc.* **1978**, *100*, 2915. (d) Braterman, P. S.; Cross, R. J.; Young, G. B. *J. Chem. Soc., Dalton Trans.* **1977**, 1892; **1976**, 1310.
(22) For example, see: (a) Smith, G.; Kochi, J. K. *J. Organomet. Chem.* **1980**, *198*, 199. (b) Ozawa, F.; Ito, T.; Nakamura, Y.; Yamamoto, A. *Bull. Chem. Soc. Jpn.* **1981**, *54*, 1868. (c) Tamaki, A.; Magennis, S. A.; Kochi, J. K. *J. Am. Chem. Soc.* **1974**, *96*, 6140. Tamaki, A.; Magennis, S. A.; Kochi, J. K. *J. Organomet. Chem.* **1972**, *40*, C81; **1973**, *51*, C39. (d) Komiya, S.; Albright, T. A.; Hoffman, R.; Kochi, J. K. *J. Am. Chem. Soc.* **1976**, *98*, 7255; **1977**, *99*, 8440. (e) Gillie, A.; Stille, J. K. *J. Am. Chem. Soc.* **1980**, *102*, 4933.
(23) Yamamoto, T.; Yamamoto, A.; Ikeda, S. *J. Am. Chem. Soc.* **1971**, *93*, 3350.
(24) Favero, G.; Turco, A. *J. Organomet. Chem.* **1976**, *105*, 389. Favero, G.; Gaddi, M.; Morvillo, A.; Turco, A. *Ibid.* **1978**, *149*, 395. Favero, G.; Morvillo, A.; Turco, A. *Ibid.* **1978**, *162*, 99.
(25) Komiya, S.; Abe, Y.; Yamamoto, A.; Yamamoto, T. *Organometallics* **1983**, *2*, 1466.

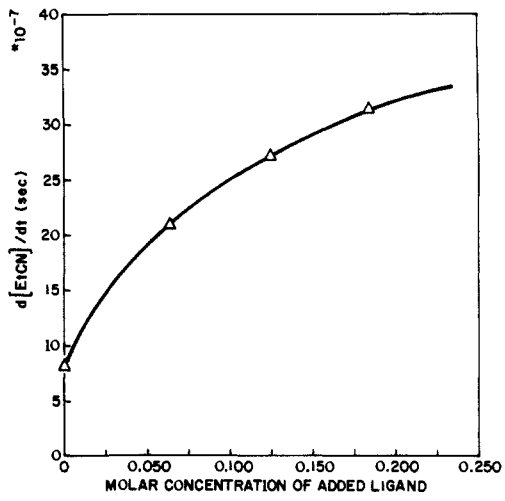

Figure 2. Rate of propanenitrile formation vs. the concentration of added ligand P(O-*o*-tolyl)$_3$ at −40 °C. [**1**] = 0.020 M in toluene-d_8.

tramolecular reductive elimination is that the eliminating groups be cis to each other.

Results and Discussion

The reaction of ethylene and hydrogen cyanide to give propanenitrile (eq 2) proceeds readily in the presence of (C_2H_4)-$L_2Ni(0)$ [L = P(O-*o*-tolyl)$_3$] (**1**) at temperatures from −60 to 0 °C. The reaction is monitored by following the appearance and

$$C_2H_4 + HCN \xrightarrow[\text{catalyst}]{Ni} CH_3CH_2CN \qquad (2)$$

disappearance of proton NMR signals of propanenitrile (0.43 ppm, t, and 1.17 ppm, q), ethylene (5.28 ppm), and hydrogen cyanide (HCN) (1.33 ppm). The position of the HCN signal is both temperature- and concentration-dependent and is not always readily identified among the signals due to catalyst. The proton NMR signals of the catalyst **1** are not altered by the presence of excess ethylene but, upon addition of ≥1 equiv of HCN, are quantitatively replaced by a new set of signals, the most characteristic of which is a broad multiplet (0.61 ppm) assigned to a Ni–C_2H_5 moiety. These signals persist until ethylene and/or HCN are consumed.

Consistent with the active participation of this Ni–C_2H_5 species in the catalytic cycle, the reaction kinetics are independent of the ethylene and HCN concentrations (0.01 to 0.25 M in each) at −40 °C. However, we were suprised to find that the reaction appeared to have second-order dependence on the initial concentration of **1** (see Figure 1) and a complex dependence on the concentration of added ligand P(O-*o*-tolyl)$_3$ (see Figure 2). A better characterization of the Ni–C_2H_5-containing intermediate was clearly necessary for mechanistic understanding.

Characterization of Catalytic Intermediate. Examination of the catalytic system by ^{31}P NMR spectroscopy reveals that upon addition of HCN in the presence of excess ethylene at −40 °C, the resonance of **1** at 141.4 ppm is quantitatively replaced by four new singlets at 129.8, 118.1, 117.7, and 116.9 ppm (see Table I) with integrated areas in a relative ratio of 1.00:0.14:0.80:0.06. The signal at 129.8 ppm is assigned to uncoordinated P(O-*o*-tolyl)$_3$ (L). These signals persist until HCN and/or ethylene are consumed. When $H^{13}CN$ is used, the three higher field signals are converted to doublets (J_{P-C} = 23, 23, 142 Hz, respectively). When $^{13}C^{12}CH_4$ is used with unlabeled HCN, the same three signals are converted to pseudotriplets, the outside lines arising from coupling to a labeled methylene of the Ni–Et moiety and the center line from nonlabeled methylene.

The ^{13}C NMR spectrum at −70 °C when $^{13}C^{12}CH_4$-enriched ethylene is used shows signals assigned to a Ni–C_2H_5 unit at 14.1 and 11.7 ppm, the latter a broad doublet with carbon–phosphorus coupling constant $J_{C-P} \cong 35$ Hz,[10] as well as a broadened signal ($\Delta\nu_{1/2}$ = 12 Hz) due to coordinated ethylene at 58.9 ppm (uncoordinated ethylene resonates at 123.4 ppm and the coordinated ethylene of **1** resonates at 47.4 ppm[26]). Coupling of the coordinated ethylene ^{13}C signal was not resolved, either to phosphorus or to ^{13}CN (using $H^{13}CN$). It is concluded that coordinated ethylene is only weakly coupled to the phosphorus and cyanide. The use of $^{13}C_2H_4$ both with and without $H^{13}CN$ also gave no useful structural information (J_{C-C} = 34 Hz in Ni–CH_2–CH_3). Signals due to Ni–*C*N were detected at 155.1, 157.9, and 155.7 ppm.

The ^1H NMR spectrum reveals a broad multiplet at 0.61 ppm assigned to the Ni–C_2H_5 group, a singlet at 2.03 ppm assigned to coordinated ethylene, and a broad singlet at 2.09 ppm assigned to the methyls of P(O-*o*-tolyl)$_3$ (L), both coordinated and uncoordinated.

On the basis of these data, the intermediate species are assigned the isomeric structures of **2a–c**. Isomer **2c** is assigned to the ^{31}P signal at 116.9 ppm on the basis of the very large coupling constant between phosphorus and cyanide. However, we have been unable to determine whether **2a** or **2b** is the major isomer because of the unexpected similarity between cis and trans coupling for P–Ni–CH_2CH_3 (see Table I). A phosphorus-decoupled ^{13}C NMR spectrum taken with $H^{13}CN$ and $^{13}C^{12}CH_4$ may distinguish between **2a** and **2b** by focussing on N*C*–Ni–*C*H_2CH_3 coupling, but we were unable to carry out this experiment.

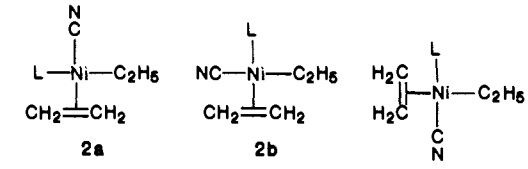

Given structures **2**, the stoichiometry of the initial reaction is as shown in eq 3. The reaction of **1** with HCN in the *absence*

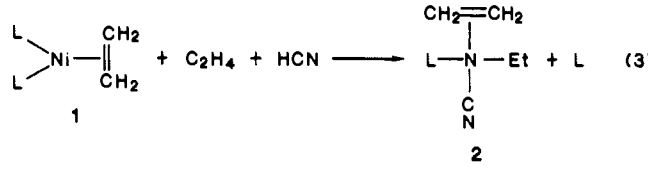

of ethylene at −40 °C still produces **2** but also produces HNi(C-N)L_3 (**3**) (eq 4), as characterized by both proton and phosphorus NMR spectra (Table I). The formation of **3** occurs even in the

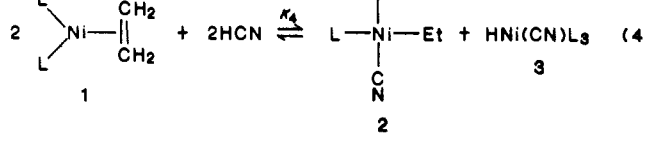

presence of ethylene when excess P(O-*o*-tolyl)$_3$ is added to the system, and it is clear from variable concentration studies that a rapid equilibration between **2** and **3** occurs with $K_5 \sim 0.1$ at −40 °C (eq 5). Therefore, **2** is the favored species even under conditions where there is less excess ethylene than P(*o*-*o*-tolyl)$_3$.

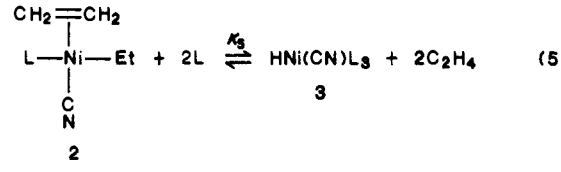

We have found that the coordinated ligand of **2** and free ligand L exchange very rapidly. With ^{31}P NMR spectroscopy, magnetization transfer (MT) techniques provide an appropriate monitor for the exchange from −90 to −60 °C since the preexchange lifetimes are comparable to the spin–lattice relaxation times (T_1) of the two sites. These experiments involves the selective

(26) Tolman, C. A.; English, A. D.; Manzer, L. E. *Inorg. Chem.* **1975**, *14*, 2353.

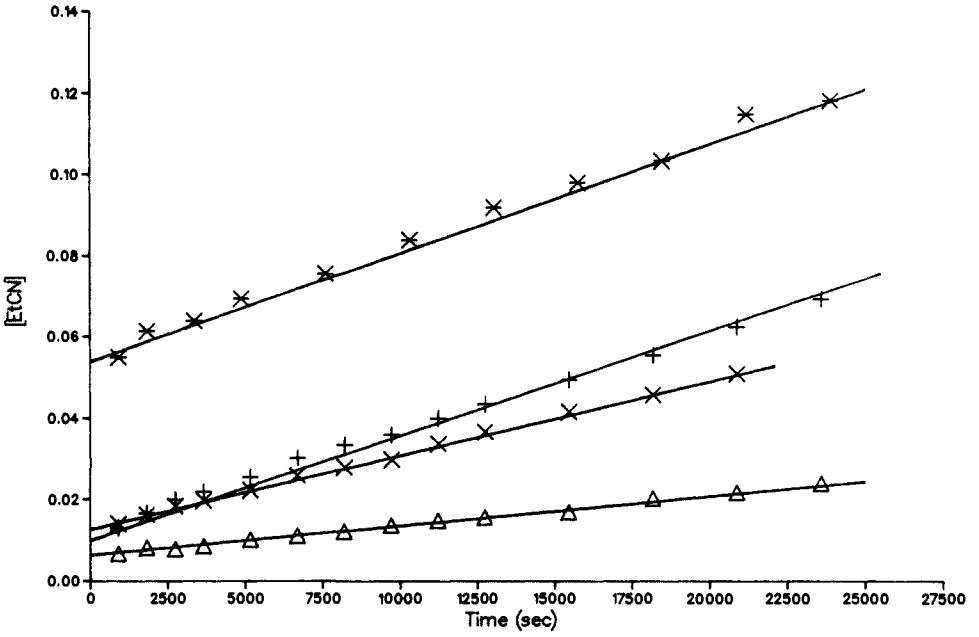

Figure 3. Theoretical fit (see text) of four sets of data with the kinetic model comprised of eq 3, 5, 6, and 7. Optimized $K_5 = 0.90 \pm 0.018$ and $K_6k_7 = 0.0050 \pm 0.0003$ L/mol·s. [1] = 0.038 M; added [L] = 0 (△), 0.065 (×), 0.130 (+), 0.195 (*), M.

inversion of one phosphorus resonance followed by a variable time delay and signal acquisition. The complementary experiment, selective inversion of the other resonance, was also performed, and the time dependence of the site intensities under both sets of conditions was analyzed to provide the exchange rates and relaxation times listed in Table IIA. These data result in the following activation parameters: $\Delta G^{\ddagger}(-75\ ^{\circ}C) = 9.7 \pm 0.1$ kcal/mol, $\Delta H^{\ddagger} = 5.2 \pm 0.3$ kcal/mol, $\Delta S^{\ddagger} = -23 \pm 13$ eu. For purposes of later comparison, we note the extrapolated $\Delta G^{\ddagger}(-40\ ^{\circ}C) = 10.5$ kcal/mol. These parameters are consistent with an associative process producing an unobserved five-coordinate intermediate **4** (eq 6). Qualitative MT experiments also suggest

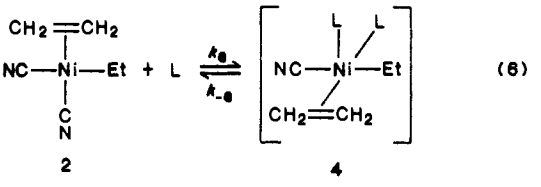

2 4 (6)

that the isomers of **2** are exchanging at a similar rate. Perhaps facile rearrangement of **4** provides a means of exchange between the isomers. Attempts to observe exchange of free ethylene with coordinated ethylene or ethyl groups were unsuccessful at −30 °C.

Kinetics of Ethylene Hydrocyanation. The apparent second-order dependence of the reaction rate on the initial concentration of **1** (Figure 1) is now readily explained as a result of the reaction (eq 3) which produces two fragments from **1**, namely **2** and L. We propose that these two fragments must recombine (eq 6) to generate a five-coordinate intermediate, **4**, which then eliminates propanenitrile and regenerates **1** (eq 7). Consistent with this

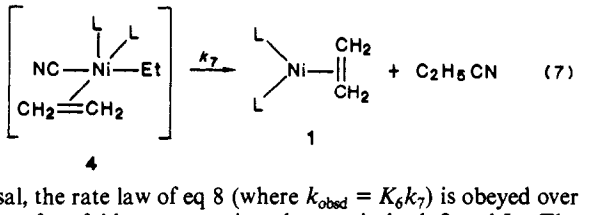

4 1 (7)

proposal, the rate law of eq 8 (where $k_{obsd} = K_6k_7$) is obeyed over a range of tenfold concentration changes in both **2** and L. The

$$d[C_2H_5CN]/dt = k_{obsd}[2][L] \quad (8)$$

nonlinear relationship between [L] and the rate shown in Figure 2 results from eq 5; at high [L] some of **2** is converted to **3** and removed from the catalytic cycle. Utilizing an iterative kinetic modeling computer program, GIT,[27] which combines statistical comparison of experimental data with a GEAR generated theoretical model, we have used a model comprised of eq 3, 5, and a combined form of 6 and 7 to optimize K_5 and K_6k_7 ($=k_{obsd}$) for four sets of concentration conditions simultaneously. The optimized values are $K_5 = 0.90 \pm 0.018$ and $K_6k_7 = 0.0050 \pm 0.0003$ L/mol·s, resulting in the fit shown in Figure 3.

Using the same model, we have determined second-order rate constants k_{obsd} over a temperature range of −10 to −50 °C using two different initial concentrations of **1** (Table IIIA). Nonlinear least-squares analysis of the temperature dependence of k_{obsd} results in the following activation parameters: $\Delta G^{\ddagger}(-40\ ^{\circ}C) = 16.7 \pm 0.1$ kcal/mol, $\Delta H^{\ddagger} = 8.8 \pm 0.9$ kcal/mol, and $\Delta S^{\ddagger} = -34 \pm 4$ eu; the large negative entropy of activation is consistent with the

Table II. Rate Constants and ^{31}P Relaxation Times from Magnetization Transfer Experiments

(A) $(C_2H_4)L(CN)(C_2H_5)Ni$ (**2**) + L $\underset{k_{-6}}{\overset{k_6}{\rightleftharpoons}}$ $(C_2H_4)L_2(CN)(C_2H_5)Ni$ (**4**)

temp (°C)	k_6[a] (L/mol·s)	T_1 (s) **2**	T_1 (s) L
−90	31	0.24	
−80	50	0.21	0.33
−70	115	0.28	0.44
−60	254	0.35	0.41

(B) $HNi(CN)L_3$ (**3**) $\underset{k_{-15}}{\overset{k_{15}}{\rightleftharpoons}}$ $HNi(CN)L_2$ (**6**) + L

temp (°C)	k_{15} (s^{-1})	T_1 (s) **3**	T_1 (s) L
−30	0.29 (0.09)[b]	0.15	0.68
−20	1.93 (0.12)[b]	0.15	0.96
	1.42 (0.04)[c]		
−10	5.35 (0.70)[b]	0.17	1.00
	6.84 (0.16)[c]		
0	22.20 (2.02)[c]	0.20	1.67

[a] $[(C_2H_4)L_2Ni, 1] = 0.026$ M in toluene/toluene-d_8. [b] $[HNi(CN)L_3, 3] = 0.050$ M in toluene-d_8; [L] = 0.050 M. [c] $[HNi(CN)L_3, 3] = 0.050$ M in toluene-d_8; [L] = 0.23 M.

(27) Weigert, F. J., private communcation. An iterative procedure is attached to a modified version of HAVCHEM obtained from Stabler and Chesnick Stabler, R. N.; Chesnick, J. *Int. J. Chem. Kinet.* **1978**, *10*, 461).

Table III. Rate Constants from NMR

(A) $C_2H_4 + HCN \xrightarrow{2} C_2H_5CN$[a]

temp (°C)	k_{obsd}[a] (L/mol·s)	temp (°C)	k_{obsd}[a] (L/mol·s)
−10	8.50×10^{-3} [b]	−40	0.92×10^{-3} [c]
−20	3.40×10^{-3} [b]		0.76×10^{-3} [b]
	3.60×10^{-3} [c]		0.64×10^{-3} [c]
−30	1.64×10^{-3} [b]	−50	0.34×10^{-3} [c]
	1.87×10^{-3} [c]		

(B) $NiL_4 + HCN \xrightarrow[3]{k_{13}} HNi(CNL)L_3 + L$[d]

temp (°C)	k_{13} (s^{-1})	temp (°C)	k_{13} (s^{-1})
−50	3.5×10^{-4}	−45	8.5×10^{-6}
−30	2.1×10^{-4}	−50	4.0×10^{-6}
−35	8.0×10^{-5}	−55	1.3×10^{-6}
−40	2.0×10^{-5}	−60	4.4×10^{-7}

[a] $d[EtCN]/dt = k_{obsd}[2][L]$. [b] $[(C_2H_4)L_2Ni, 1] = 0.048$ M in toluene-d_8. [c] $[(C_2H_4)L_2Ni, 1] = 0.020$ M in toluene-d_8. [d] $d[3]/dt = k_{13}[NiL_4]$; initial conditions, $[NiL_4] = 0.040$ M in toluene-d_8.

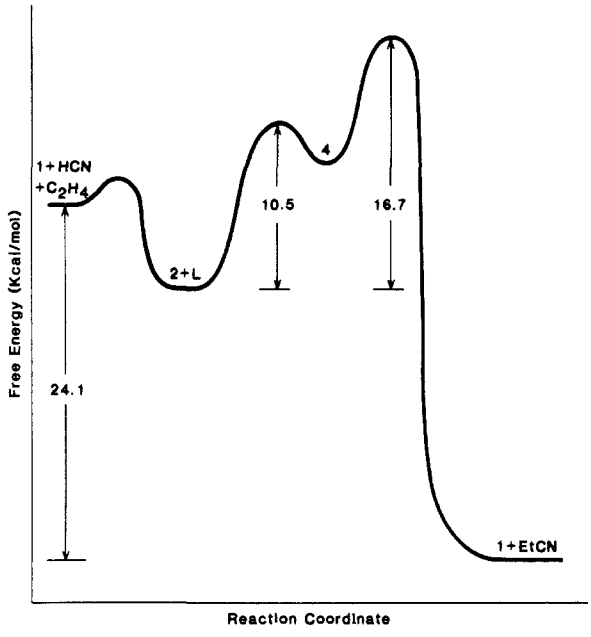

Figure 4. Reaction coordinate diagram illustrating the free energy relationships for converting HCN and C_2H_4 to propanenitrile in the presence of $(C_2H_4)L_2Ni$, **1**.

formation of a five-coordinate intermediate prior to reductive elimination.

Figure 4 shows a proposed reaction coordinate illustrating the relationship of the free energy of activation at −40 °C for ligand exchange in **2** (10.5 kcal/mol) with that of the production of propanenitrile (16.7 kcal/mol). The free energy of formation of propanenitrile from ethylene and hydrogen cyanide at −40 °C is 24.1 kcal/mol.[28] The fact that the formation of **2** from **1** is very rapid compared to the production of propanenitrile suggests that the starting point energy is well below the transition-state energy as illustrated. Unfortunately, the depth of the valleys cannot be determined from the current data, though **2** + L must be at least several kcal/mol below **1** + HCN + C_2H_4 because **1** is not observed under these condition; likewise, **4** is not observed.

Equilibrium Studies. Preliminary kinetic experiments were marked by the erratic appearance of L_4Ni at concentrations which depended upon the detailed prior history of the sample. These observations indicated the presence of a variety of equilibria which were unproductive in terms of the catalytic cycle. The principal features of these equilibria are described below and lead to a description linking the "unproductive" species to the key catalytic intermediates.

Table IV. Equilibrium and Thermodynamic Data[a]

temp (°C)	K_{eq}	ΔH (kcal/mol)	ΔS (eu)	ΔG(−40 °C) (kcal/mol)
(A) $(C_2H_4)L_2Ni + L \rightleftharpoons (C_2H_4)L_3Ni$				
−30	1.5×10^2			
−40	5.0×10^2	−12.7 ± 1.0	−42 ± 8	−2.9
−50	1.6×10^3			
−60	5.8×10^3			
(B) $L_4Ni \rightleftharpoons L_3Ni + L$				
65	2.27			
55	1.03			
45	0.45			
40	0.27			
35	0.19	17.0 ± 0.5	52 ± 5	4.9
30	0.11			
20	0.044			
15	0.031			
10	0.015			
0	0.0057			
(C) $L_4Ni + C_2H_4 \rightleftharpoons (C_2H_4)L_3Ni + L$				
−30	3.5			
−40	5.0	−4.1 ± 1.0	−14 ± 10	−0.8
−50	6.7			
−60	11.9			

[a] In toluene-d_8; L = P(O-*o*-tolyl)$_3$.

Equilibria Involving $(C_2H_4)L_2Ni(0)$ (1). Complex **1** reacts with 1 equiv of P(O-*o*-tolyl)$_3$, L, at −40 °C to produce the novel species $(C_2H_4)L_3Ni(0)$, **5** (eq 9), which has been characterized by ^{31}P and ^1H NMR spectroscopy (see Table I). To our knowledge, this is the first direct observation of an L_3Ni(olefin) complex with monodentate ligands.[29] The equilibrium (eq 9) strongly favors **5** at low temperatures (see Table IVA), but as the temperature is increased, entropic effects dominate and the equilibrium shifts

$$\underset{\mathbf{1}}{(C_2H_4)L_2Ni} + L \rightleftharpoons \underset{\mathbf{5}}{(C_2H_4)L_3Ni} \quad (9)$$

to favor **1**, such that at 0 °C complex **1** is the major species. This temperature dependence explains why Tolman and Seidel[4] observed only **1** at ambient temperature.

As mentioned above, the presence of excess ethylene causes no change in either the phosphorus or proton NMR spectrum of **1**. Yet Tolman and Seidel[4,5] established that olefin exchange in **1** and related species proceeds by an associative process and found evidence for bis-olefin complexes (as illustrated in eq 10) at very high olefin concentrations. Consistent with these observations,

$$(CH_2{=}CHR)L_2Ni + CH_2{=}CHR \rightleftharpoons (CH_2{=}CHR)_2NiL_2 \quad (10)$$

^{31}P and ^1H NMR of a sample charged with 800 psi of ethylene indicate the presence of at least four species which exhibit dynamic behavior even at −140 °C. Since these species are observed only in the presence of a large excess of ethylene (the solution is approximately 10 M C_2H_4), the equilibrium constants for their formation must be at least 10^4 smaller than that for eq 9. Under the conditions of the kinetic experiments ($[C_2H_4] = 0.20$ M) it seems probable that the bis-ethylene complex is present at such low concentration that the resonance assigned to **1** does in fact represent $(C_2H_4)L_2Ni$ alone rather than an exchange averaged signal involving eq 10.

Equilibria Involving L_4Ni and L_3Ni. The 18-electron complex L_4Ni is, for the most part, inert toward associative processes (protonation is an exception) and therefore must dissociate ligand to generate the very reactive 16-electron complex L_3Ni (eq 11) to participate in catalytic activity.[10,30] When L = P(O-*o*-tolyl)$_3$,

$$L_4Ni \rightleftharpoons L_3Ni + L \quad (11)$$

(28) Stull, D. R.; Westrum, E. J., Jr.; Sinke, G. C. *The Chemical Thermodynamics of Organic Compounds*; John Wiley & Sons, Inc.; New York, 1969.

(29) For (triphos)Ni(C_2F_4) see: Browning, J.; Penfold, B. R. *J. Chem. Soc., Chem. Commun.* **1973**, 198.

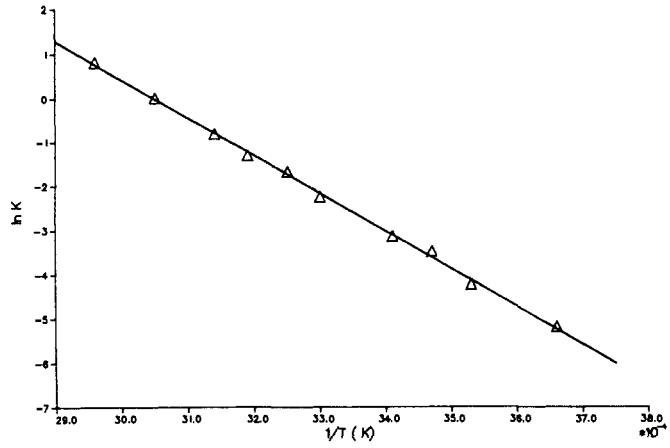

Figure 5. Plot of ln K vs. $1/T$ $(K)^{-1}$ for $NiL_4 \rightleftharpoons NiL_3 + L$, see Table IVB.

the equilibrium (eq 11) favors the L_3Ni species at ambient temperature and above. Previous measurements of this equilibrium were obtained with use of UV–vis spectrophotometry; only the L_3Ni species is observable by this technique.[2] We have reexamined this equilibrium using ^{31}P NMR spectroscopy whereby all three components may be measured directly. Equilibrium constants for the temperature range 0–65 °C are given in Table IVB (see Figure 5), along with thermodynamic parameters. The ΔH and ΔS values are somewhat greather than those previously reported (earlier estimates are ΔH = 13 kcal/mol; ΔS = 37 eu);[2] presumably the NMR results are more accurate because all components are being monitored.

The reaction of L_4Ni with ethylene displaces L to produce **5** at low temperatures (eq 12). Equilibrium data from −30 to −60 °C are given in Table IV with thermodynamic parameters.

$$L_4Ni + C_2H_4 \rightleftharpoons \underset{\mathbf{5}}{(C_2H_4)L_3Ni} + L \qquad (12)$$

The reaction of L_4Ni with HCN at −40 °C produces the hydridonickel cyanide complex **3** (eq 13).[3] The equilibrium heavily favors **3** even with a large excess of L and only a stoichiometric amount of HCN; at −40 °C, $K_{eq} \simeq 10^3$.

$$L_4Ni + HCN \rightleftharpoons \underset{\mathbf{3}}{HNi(CN)L_3} + L \qquad (13)$$

It follows from these results then that L_3Ni prefers to coordinate ethylene over L by about a factor of 5 at −40 °C, whereas reaction of HCN is favored over L by a factor of 10^3.

In comparing these equilibria, it is interesting to note that the addition of L to L_3Ni proceeds much more slowly than the addition of either ethylene or HCN; at −40 °C, the addition L to L_3Ni takes hours to equilibrate whereas with either ethylene or HCN equilibrium is achieved in a matter of minutes. It follows that the dissociation of L from L_4Ni is also relatively slow and complicates the kinetics of propanenitrile production.

Kinetics of L_4Ni Dissociation. Tolman, Seidel, and Gosser[7] found that the rate of dissociation of L from L_4Ni was independent of the reagent used to trap the resulting L_3Ni intermediate for a variety of aromatic phosphite ligands. We assumed that this would be true when L = $P(O\text{-}o\text{-}tolyl)_3$ as well, and because of the very strong thermodynamic preference for the reaction of HCN with L_3Ni, we chose to follow the forward reaction of eq 13 by ^{31}P NMR spectroscopy. Indeed we found that the reaction rate is independent of the HCN concentration and follows the rate law

$$d[3]/dt = k_{13}[L_4Ni] \qquad (14)$$

Therefore the forward rate of eq 11 is being measured. Rate constants were obtained over the temperature range −60 to −25 °C (see Table IIIB). Nonlinear least-squares analysis of these

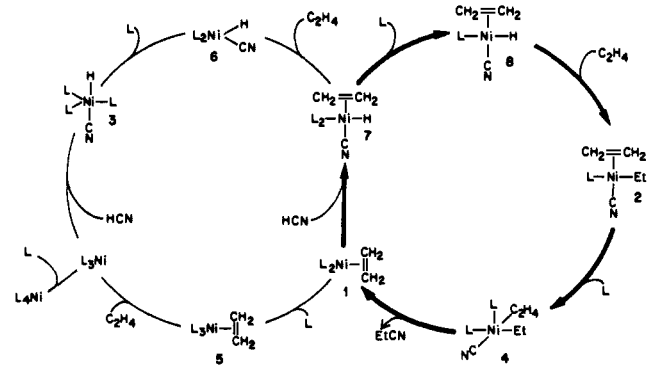

Figure 6. Proposed mechanism of ethylene hydrocyanation including nonproductive equilibria.

data resulted in the following activation parameters for k_{13}: $\Delta G^{\ddagger}(-40\ °C)$ = 18.4 ± 0.1 kcal/mol, $\Delta H^{\ddagger}$ = 20.1 ± 1.6 kcal/mol, and $\Delta S^{\ddagger}$ = 7 ± 7 eu. Therefore, the activation energy for L dissociation from L_4Ni is higher than that of the catalytic rate limiting step.

Kinetics of Dissociation of L from $HNi(CN)L_3$ (3). In contrast to the relatively slow dissociation of L from L_4Ni, the dissociation of L from **3** (eq 15) is rapid, as qualitatively indicated by its

$$\underset{\mathbf{3}}{HNi(CN)L_3} \underset{k_{-15}}{\overset{k_{15}}{\rightleftharpoons}} \underset{\mathbf{6}}{HNi(CN)L_2} + L \qquad (15)$$

equilibration with **2** (eq 4). An upper bound to the dissociation rate is immediately suggested by the absence of exchange-induced line broadening in the ^{31}P NMR spectrum of **3** in the presence of L at temperatures below 10 °C. The thermal instability of **3** precludes rate measurements by line shape analysis at temperatures sufficient to approach coalescence. Again, magnetization transfer techniques were found to provide an appropriate monitor for the exchange from −40 to 0 °C.

The exchange rates and relaxation times are listed in Table IIB. The activation parameters for ligand dissociation estimated from these rate constants (k_{15}) are $\Delta H^{\ddagger}$ = 18.8 ± 2.6 kcal/mol, $\Delta S^{\ddagger}$ = 17 ± 7 eu, and $\Delta G^{\ddagger}(-40\ °C)$ = 14.8 ± 0.5 kcal/mol. These values may be compared with those previously obtained for $HNi(PEt_3)_3CN$ ($\Delta H^{\ddagger}$ = 15.1 kcal/mol, $\Delta S^{\ddagger}$ = 10.3 eu, and $\Delta G^{\ddagger}(-40\ °C)$ = 12.7 kcal/mol) with line shape analysis.[3]

Mechanism of Ethylene Hydrocyanation. The mechanistic scheme illustrated in Figure 6 is consistent with the accumulated experimental data. The bold cycle on the right-hand side is the productive catalytic cycle whereas the cycle on the left side shows various equilibria which can remove nickel from the productive catalytic loop: all steps except the one step which produces propanenitrile are reversible; no evidence for oxidative addition of propanenitrile to **1** has been found.

The addition of HCN to the 16-electron complexes **1** is apparently very rapid, similar to the extremely rapid addition of HCN to the 16-electron complex L_3Ni. The HCN adduct **7** then may either dissociate L and add ethylene to produce **2** (bold cycle) or dissociate ethylene and add L to give **3**.

The very rapid equilibration rates measured between **3** and **6** (eq 14) lead us to expect that the rates of equilibration between **6** and **7** and between **7** and **8** are of similar magnitude. The conversion of **8** to **2** involves both ethylene association and ethylene insertion into Ni–H; we expect that association occurs first because primary insertion would create a very unlikely 14-electron intermediate.[30] We cannot rule out the possibility that **7** will insert coordinated ethylene into the Ni–H bond before other ligand exchange occurs. The rapid equilibration between **2** and **3** is proposed to take place through the upper half of the two cycles.

The final reductive elimination step occurs from the five-coordinate complex **4** which is produced in a rapid equilibration involving the addition of L to **2**; the equilibrium heavily favors **2**.

The erratic presence of L_4Ni in the kinetic experiments is a result of the equilibria in the lower part of the left-hand cycle.

(30) Tolman, C. A. *Chem. Soc. Rev.* **1972**, *1*, 337.

We have shown that the equilibria between **1** and **5** and between **5** and L_3Ni are rapidly maintained but that the equilibrium between L_4Ni and L_3Ni is achieved very slowly. In our initial studies, we prepared samples by adding L to **1** and cooling to −80 °C. After a variable period of time, HCN and then ethylene were added, and the sample was warmed to reaction temperature, e.g., −40 °C. This procedure allowed the production of varying amounts of L_4Ni which was then very slow to dissociate L and reenter the catalytic cycle. If, on the other hand, ethylene is added before the sample is cooled, the equilibrium preference for **5** over L_4Ni keeps all of the nickel available in the catalytic cycle. All subsequent experiments were carried out by saturating the catalytic mixture with ethylene prior to cooling, and the erratic presence of L_4Ni was eliminated.

To our knowledge, the only other study of organonitrile reductive elimination is reported by Favero et al.[24] as shown in eq 16. On the surface, it also looks like an associative process; the

$$L_2Ni(Ph)(CN) + L' \rightarrow L_2NiL'_2 + PhCN \qquad (16)$$

$$L = PEt_3;\ L' = P(OEt)_3$$

complex is stable in the absence of $P(OEt)_3$. However, addition of PEt_3 generates an $L_3Ni(Ph)(CN)$ species which is also stable toward elimination of PhCN. We are reexamining this system and have found that the initial step is the substitution of $P(OEt)_3$ for PEt_3; the coordination number of the actual elimination complex is not yet clear.[31]

Considering the relatively few well-documented cases of associative reductive elimination, it is interesting to note that a recent theoretical study[32] has suggested that reductive elimination from a dialkylnickel species should be more easily accomplished from a five-coordinate species such as L_3NiR_2 or $L_2(olefin)NiR_2$ rather than from four-coordinate species. This preference is primarily a result of the relative stability of the generated nickel fragment NiL_3 or $(olefin)NiL_2$ vs. a 14-electron NiL_2. In our case, the generated fragment is the isolable complex **1**, whose stability must contribute greatly to the driving force of the reaction.

In closing, we note a structural relationship between our proposed five-coordinate intermediate **4** and a five-coordinate intermediate proposed by Ozawa, Ito, and Yamamoto[33] during the β-hydride elimination depicted in eq 17. This intermediate is

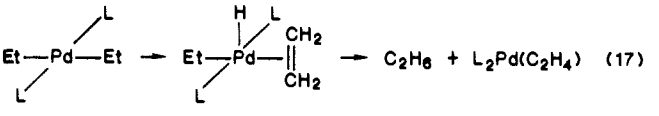

(17)

strikingly similar to **4** (eq 6) if hydride is replaced by cyanide and results in essentially the same elimination products.

Experimental Section

All synthetic procedures and sample preparations were carried out in a Vacuum Atmosphere drybox. The complex $(C_2H_4)L_2Ni$ (**1**) was prepared according to literature methods.[34] L_4Ni may be prepared by literature methods[2b] or by treating **1** with an excess of L in toluene, reducing the volume under reduced pressure, adding acetonitrile and cooling to −25 °C. The white crystalline product was washed with acetonitrile and dried under high vacuum. $P(O\text{-}o\text{-}tolyl)_3$ was prepared from PCl_3 and *o*-cresol according to literature methods.[35] Hydrogen cyanide was purchased from Fumico Inc. (Amarillo, TX) and was distilled to remove acidic inhibitors prior to use.

Caution! Hydrogen cyanide (HCN) is very volatile and highly toxic[36] and should be used only in a well-ventilated fume hood or drybox. Distilled HCN is also prone to very exothermic oligomerization when warmed and should be kept at 0 °C or lower at all times.

Typical sample preparation involved dissolving **1** in toluene-d_8 and charging a screw cap 5-mm NMR tube. $P(O\text{-}o\text{-}tolyl)_3$ was added and the sample saturated with ethylene by sparging through a long needle. The sample was sealed with the septum screw cap and cooled to −80 °C in a dry ice–acetone bath. A cold 25% HCN/CH_2Cl_2 solution was then injected by microliter syringe; the HCN freezes on the side of the tube until mixing was initiated at the time of the kinetic run. The CH_2Cl_2 becomes an internal standard for the proton NMR spectra.

NMR spectra were obtained on Nicolet NT-360 instrument at 360.961 MHz for protons, at 146.14 MHz for phosphorus, and at 90.80 MHz for carbon. Some phosphorus spectra were obtained on a Nicolet 300 MHz instrument operating at 121.68 MHz. T_1 measurements of all species were measured at appropriate temperatures and pulse delays set accordingly. Chemical shifts are reference to tetramethylsilane (Me_4Si) for proton and carbon spectra and to external phosphoric acid for phosphorus spectra. Magnetization transfer experiments were performed by attenuating the low-power transmitter such that a selective inversion pulse was obtained in 2–5 ms. Both the experimental technique and method of analysis have been described previously.[37] The high-pressure experiments were conducted in a sapphire NMR tube which is capable of withstanding several thousand psi.

Acknowledgment. We thank Drs. Todd Marder and William Seidel for helpful discussions and George Watunya for technical assistance.

(31) McKinney, R. J.; Fox, L.; Roe, D. C., unpublished results.
(32) Tatsumi, K.; Nakamura, A.; Komiya, S.; Yamamoto, A.; Yamamoto, T. *J. Am. Chem. Soc.* **1984**, *106*, 8181.
(33) Ozawa, F.; Ito, T.; Yamamoto, A. *J. Am. Chem. Soc.* **1980**, *102*, 6457.
(34) Seidel, W. C.; Tolman, C. A. *Inorg. Chem.* **1970**, *9*, 2354.
(35) Walsh, E. N. *J. Am. Chem. Soc.* **1959**, *81*, 3023.
(36) For additional details, see: *Prudent Procedures for Handling Hazardous Chemicals in Laboratories*; National Academy Press: Washington, D. C., 1981; pp 45–47.
(37) Alger, J. R.; Prestegard, J. H. *J. Magn. Reson.* **1977**, *27*, 137.